

## The Structure of the *I* Phase, $V_{41}Ni_{36}Si_{23}$ , a Pseudo Superstructure\*

BY CLARA BRINK SHOEMAKER AND DAVID P. SHOEMAKER

Department of Chemistry, Oregon State University, Corvallis, Oregon 97331, USA

(Received 26 March 1980; accepted 9 September 1980)

### Abstract

The *I* phase,  $V_{41}Ni_{36}Si_{23}$ , is monoclinic,  $a = 13.462$  (6),  $b = 23.381$  (9),  $c = 8.940$  (4) Å,  $\beta = 100.34$  (4)°, 228 atoms per unit cell, space group *Cc* ( $C_2^c$ ). Almost all strong reflections have  $k = 3n$ , indicating a pseudo superstructure. Structure models were obtained with *MULTAN* in space group *C2/c*, which could not be refined. A Fourier synthesis in space group *Cc*, phased by a group of atoms common to these models, yielded with small changes a model which refined by full-matrix least squares to  $R_w(F) = 0.08$  for all 4065 reflections. The structure may be visualized as a stacking in the *b* direction of 12 ruffled layers consisting of pentagons and triangles creating a pseudo repeat of  $\frac{1}{3}b$  and many pseudo symmetry elements. The asymmetric unit comprises three of these layers, with their associated 'subsidiary' atoms. The structure is ideally 'tetrahedrally close-packed' (t.c.p.) with V in the 12 CN 16, the 6 CN 15 and the 6 CN 14 positions. Eighteen Ni and eleven Si are ordered in 29 of the 33 CN 12 positions and a mixture of Ni and Si occurs in the remaining four CN 12 positions. Si–Si contacts do not occur; however, a few contacts occur between positions occupied by Si and mixtures. Contacts of the latter type were not found in t.c.p. structures containing less Si (*v*, *X*, *K*, and *R* phases). The coordination distances cover a range of 2.12–3.02 Å and depend in the same way on CN as found for other t.c.p. structures.

### Introduction

The *I* phase was discovered by Bardos & Beck (1966) in the V–Ni–Si system at 1373 K and by Bardos, Malik, Spiegel & Beck (1966) in the Mn–Co–Si and Mn–Ni–Si systems at 1273 K. Kuzma & Hladyshevskii (1964) and Kuzma, Hladyshevskii & Cherkashin (1964) have reported a phase, which they called the *S* phase, in the Mn–Co–Si and the

Mn–Ni–Si systems at 1073 K at approximately the *I* phase compositions. In an earlier publication (Shoemaker & Shoemaker, 1967) we concluded from a comparison of the powder diagrams that the *I* phase and the *S* phase are probably isostructural. With the aid of single-crystal intensities from a very small crystal fragment we indexed the powder diagram of the *I* phase ( $V_{41}Ni_{36}Si_{23}$ ) on a large monoclinic cell with cell dimensions:  $a = 13.403$ ,  $b = 23.336$ ,  $c = 9.129$  Å,  $\beta = 99.11$ °,  $Z = 230$  atoms per cell, space group *C2/c* or *Cc*. A possible relationship with the  $\mu$  phase was discussed, but in view of the low quality of the crystal fragments and the complexity of the problem no further structure determination was attempted at that time. More recently, as part of our study of transition-metal intermetallic compounds with Si, we have resumed our work on the structure of the *I* phase, having succeeded in finding better crystal specimens. Previously we found that these silicon-containing structures are still ideally tetrahedrally close-packed (t.c.p.) up to 19 at.% Si (*K* phase:  $Mn_{77}Fe_4Si_{19}$ , Shoemaker & Shoemaker, 1977), whereas in the *D* phase with 29 at.% Si ( $Mn_5Si_2$ , Shoemaker & Shoemaker, 1976) some irregular coordinations occur. The study of the *I* phase was of interest because its Si content (up to 27 at.%) lies between that of the *K* and the *D* phases. Kripyakevich & Yarmolyuk (1970) have found that the *C* phase ( $V_{40}Co_{34}Si_{26}$ ) with 26 at.% Si is still ideally t.c.p., but the distribution of the Co and the Si atoms was not determined in that study.

### Experimental

An irregular crystal fragment of dimensions 0.033–0.054 mm was used for the collection of intensity data with Mo  $K\alpha$  radiation on an automated Syntex *P1* diffractometer equipped with a graphite monochromator. A  $\theta$ – $2\theta$  scan was used; the scan speed was 1° min<sup>-1</sup>, the  $2\theta$  range was 2.0° plus the  $\alpha_1\alpha_2$  angular separation. Background readings were made at the beginning and the end of each scan range; the ratio of background time to scan time was 1 to 2. The

\* Research supported by National Science Foundation Grant DMR 76-80559.

Table 1. *Crystal data for the I phase,  $V_{41}Ni_{36}Si_{23}$* 

FW/100	48.48	Space group	$Cc(C_2^1)$
<i>a</i> (Å)	13.462 (6)	Atoms/cell	$4 \times 57 = 228$
<i>b</i> (Å)	23.381 (9)	$D_m$ (Mg m <sup>-3</sup> )	6.59 (6)
<i>c</i> (Å)	8.940 (4)	$D_x$ (Mg m <sup>-3</sup> )	6.63
$\beta$ (°)	100.34 (4)	$F(000)/2$	2600
$V$ (Å <sup>3</sup> )	2768.6 (2.1)	$\mu$ (Mo <i>K</i> $\alpha$ ) (mm <sup>-1</sup> )	21.9
$\lambda$ (Mo <i>K</i> $\alpha$ ) (Å)	0.710688		

reflections in a quarter sphere of reciprocal space were measured out to  $2\theta = 60^\circ$ . No correction for absorption was made; the average value for  $\mu r = 0.48$ . In a later stage of the refinement a secondary-extinction correction factor was applied in the form  $F_o^{corr} = F_o(1 + gI_o)$  (Zachariasen, 1963). The value of *g* was refined with the least-squares program *NUCLS*; the largest correction was 6% for the 204 reflection.

The crystal data are given in Table 1. The cell dimensions, especially *c*, are significantly different from those determined earlier (see above), since several lines in the powder diagram were misindexed due to the large cell dimensions. A table of the observed powder pattern, and that calculated (by the program of Yvon, Jeitschko & Parthé, 1969) for the cell dimensions listed in Table 1 and the refined atom parameters, has been deposited.\*

### Structure determination

Direct methods are not expected to work well for the t.c.p. structures in which the dense packing of atoms causes a very non-statistical distribution of intensities in reciprocal space. Nevertheless, the symbolic-addition direct sign-determining method was used successfully in the structure determination of the *X* phase ( $Mn_{44}Co_{40}Si_{15}$ ; Manor, Shoemaker & Shoemaker, 1972). An additional problem in the case of the *I* phase is the predominance of strong reflections with  $k = 3n$ . The structure is not a straightforward superstructure of a subcell with *b* divided by three, since some very strong reflections occur with  $k \neq 3n$ . An attempt was made to solve the structure with the program *MULTAN* (Main, Hull, Lessinger, Germain, Declercq & Woolfson, 1978) in space group  $C2/c$ , with 300 *E* values  $> 1.8$  and 2000 phase relationships. The intensity statistics indicated the structure to be hypercentric. Two reflections with  $k \neq 3n$  were used in the starting set of five. None of the eight phase sets generated had outstanding figures of merit, but two structure models were derived, not very different from each other,

having atoms with recognizable coordination polyhedra and reasonable distances. Neither model refined by least squares to an *R* factor below 36% for 900 low-order reflections with  $I > 2\sigma$ . Not surprisingly, the coordinates of all of the atoms in the models occurred in groups of three, with *y* values differing by about  $\frac{1}{3}$ . An attempt to renormalize the *E*'s, such that  $\bar{E}^2 = 1$  separately for groups of reflections with  $k = 3n$  and  $k \neq 3n$ , led to *E* maps with many small peaks too close together.

The structure models in  $C2/c$  were then examined more closely. The coordination polyhedra of atoms close to a twofold axis could be made more regular by dropping this axis. An asymmetric structure fragment of 19 atoms (including an atom on the original twofold axis) was derived, common to both  $C2/c$  models, and comprising the total surroundings of five atoms (four icosahedra and one CN 15). A Fourier synthesis based on this fragment in space group *Cc* showed peaks closely corresponding to the positions of the atoms in one of the trial models. This structure now had 57 non-equivalent atoms in fourfold general positions (27 pairs of atoms + 3 atoms that were on original twofold axes), leading to 170 parameters (positions + scale). Six least-squares cycles on 876 low-order reflections (including all the weak ones, and the few with negative intensities allocated a small positive value) with unit weights to emphasize the contributions of the weak reflections, and an average scattering factor for all the atoms, led to  $R_w = 0.185$  and  $R = 0.266$ . The interatomic distances at this point were rather good, except for atom 13' (primed atoms are related to unprimed ones by a twofold axis in the centrosymmetric model), which had distances too small and too large. A projection of part of the structure down the *b* axis revealed an icosahedral hole (defined by 12 atoms not including atom 13') with its center about 2.5 Å from atom 13'. This atom was therefore replaced by atom 13\* centering the icosahedral hole. All atoms had now the 'normal' coordinations (CN 16, CN 15, CN 14 and CN 12) of ideally t.c.p. structures. In this final model atom 13 and its surroundings corresponded with atoms in one of the centrosymmetric models, and atom 13\* and its surroundings were present in the other centrosymmetric model. Thus, the final structure is a kind of combination of the two centrosymmetric models.

### Structure refinement

The refinements were carried out on the Lawrence Berkeley Laboratory CDC 7600 computer from a remote terminal with the *LESQ* and the *NUCLS* programs contained in Zalkin's *XRAY 76* program system. The scattering factors for the neutral atoms were taken from *International Tables for X-ray Crystallography* (1962) and corrected for the real and

\* Tables of observed and calculated powder patterns, structure factors and interatomic distances, and Fig. 2 in stereoscopic form, have been deposited with the British Library Lending Division as Supplementary Publication No. SUP 35634 (27 pp.). Copies may be obtained through The Executive Secretary, International Union of Crystallography, 5 Abbey Square, Chester CH1 2HU, England.

imaginary parts of the anomalous dispersion (Cromer & Liberman, 1970). After two initial cycles with unit weights, weights were derived from the standard errors in the intensities  $I_o$  as estimated with the equation  $\sigma(I_o) = [C + Bt^2 + (0.03C)^2]^{1/2}$  ( $C$  is the integrated count,  $B$  is the total background count,  $t = 2$  is the ratio of the scan time over the background time). In the first five cycles (two with all the data, then three with only  $I > 2\sigma$ ) the positional parameters (minus 2 to fix the origin), the scale factor, and 56 occupancy factors were varied — 226 parameters in all — with the  $V$  scattering factor for all the atoms. This showed that all atoms with  $CN > 12$  were essentially  $V$ , and that some  $CN = 12$  atoms were  $Ni$  and others  $Si$ . From then on the three scattering factors were used, and two more cycles with all the data were run varying positions and  $B$ 's, followed by two cycles varying positions and occupancies ( $m$ 's). From here on the  $m$ 's of the  $V$  atoms were set at unity and not varied further except for atom 19' ( $CN$  15) which had a negative  $B$  and for four of the six  $CN$  14 atoms. The occupancies of the  $Ni$  and  $Si$  atoms were set at unity and not varied further, except for  $Si$  atoms 5, 20' and 28' which had respectively low occupancy, high  $B$  and negative  $B$ . Four  $CN$  12 positions had scattering factors intermediate between those for  $Ni$  and  $Si$ . They were assumed to be occupied by mixtures of  $Ni$  and  $Si$ ; they were given the  $V$  scattering factor (between  $Ni$  and  $Si$ ) and their  $m$ 's were varied. Three cycles were thus run with 239 parameters (169 positional, 1 scale, 57  $B$  and 12  $m$ ). Two more cycles varying positions, scale and  $B$  led to the agreement factors of Table 2 and the final parameters of Table 3. The range of interatomic distances is given in Table 4. The table of structure-factor agreement and the complete table of interatomic distances have been deposited.\* The value of  $S$  for the whole data set is close to one, which is consistent with a basically correct model and an appropriate weighting scheme. (An additional cycle with the sign of  $f''$  reversed resulted in small but insignificant increases in  $R$ ,  $R_w$ , and  $S$ .)

The large percentage of weak reflections (59% smaller than  $2\sigma$ ) limits the accuracy of the analysis and results in rather high standard deviations in the parameters, as well as giving a large value of  $R$ . The

\* See previous footnote.

Table 2. Agreement factors for the least-squares refinements of the  $I$  phase

Number of reflections	Number of variables	$R(F)$	$R_w(F)$	$S^*$
4065	227	0.227	0.080	1.058
1674 ( $I > 2\sigma$ )	227	0.079	0.064	1.361

$$* S = [\sum w(F_o - F_c)^2 / (n_{ref.} - n_{var.})]^{1/2}.$$

Table 3. Atomic parameters for the  $I$  phase (coordinates  $\times 10^4$ )

All atoms are in 4(a). Atoms with roughly the same  $x$  and  $z$  values and with  $y$  values separated by roughly  $\frac{1}{2}$  are grouped together. Note that atoms 22', 27 and 15' are listed twice, as each appears to fit into two different groups; the listing with the poorer fit is in parentheses. Note that atom 13\* is listed with two of the duplicated atoms. The occupancies ( $m$ ) are as follows: atom 19' 1.01 (4), 3' 0.88 (3), 14 0.95 (13), 20' 1.00 (13), 25' 0.74 (6), 16' 1.14 (4), 27 1.05 (4), 15' 1.01 (4), 14' 1.11 (5), 23 1.03 (5); remaining atoms 1.00. The %  $Si$  for atoms 3', 14, 25' and 16' are 56., 45., 79. and 13. respectively.

Atom	CN	Occu-pancy	$x$	$y$	$z$	$B$ ( $\text{\AA}^2$ )	$f_o$
2	12	Ni	4978	0278 (3)	2398	0.02 (8)	28.
29	12	Ni	4642 (6)	3728 (3)	2329 (10)	0.46 (10)	28.
30	12	Ni	4643 (6)	6839 (3)	2409 (10)	0.40 (9)	28.
1	15	V	3957 (8)	0306 (4)	4928 (13)	0.42 (14)	23.
19	16	V	3825 (8)	3671 (4)	4871 (13)	0.16 (14)	23.
18'	15	V	3823 (8)	6889 (4)	4866 (13)	0.48 (14)	23.
1'	16	V	5779 (8)	0287 (4)	9960 (12)	0.25 (12)	23.
19'	15	V	5564 (7)	3675 (3)	9886 (12)	-0.17 (12)	23.2
18	15	V	5582 (8)	6922 (4)	9873 (13)	0.16 (13)	23.
3'	12	Ni, Si	5582 (10)	0839 (5)	4408 (17)	0.20 (12)	20.2
14	12	Ni, Si	5530 (10)	4176 (5)	4499 (15)	0.32 (11)	21.8
21'	12	Ni	5463 (7)	7431 (3)	4499 (10)	0.50 (10)	28.
4	12	Ni	4032 (7)	0544 (3)	7843 (10)	0.47 (10)	28.
22'	14	V	3772 (8)	4078 (4)	7872 (13)	0.75 (14)	23.
26'	12	Ni	3907 (6)	7189 (3)	7813 (10)	0.35 (10)	28.
4'	12	Si	5651 (14)	0593 (7)	7035 (22)	1.18 (27)	14.
22	12	Si	5671 (13)	3922 (7)	6937 (20)	1.11 (26)	14.
26	12	Si	5473 (12)	7163 (7)	7123 (18)	0.46 (22)	14.
5	12	Si	3236 (12)	0319 (6)	1967 (17)	0.02 (17)	14.
20'	12	Si	2909 (21)	3640 (13)	1947 (30)	3.35 (49)	14.0
25'	12	Ni, Si	3007 (8)	6962 (5)	1913 (13)	-0.14 (17)	17.0
5'	16	V	7010 (8)	0310 (4)	3033 (13)	0.42 (12)	23.
20	12	Ni	6468 (7)	3644 (3)	2864 (10)	0.36 (10)	28.
25	12	Ni	6483 (6)	6929 (3)	2876 (10)	0.15 (9)	28.
8	12	Ni	9585 (6)	0306 (3)	0994 (10)	0.38 (10)	28.
7	16	V	9116 (8)	3596 (4)	0817 (12)	0.26 (13)	23.
11	16	V	9081 (8)	6969 (4)	0849 (13)	0.41 (14)	23.
8'	15	V	0544 (8)	0280 (5)	4004 (14)	0.88 (15)	23.
7'	16	V	0357 (9)	3582 (4)	3935 (14)	0.54 (15)	23.
11'	16	V	0335 (8)	7035 (4)	3975 (12)	0.21 (13)	23.
10	16	V	2345 (7)	0313 (4)	9023 (11)	0.07 (11)	23.
12'	15	V	2148 (8)	3578 (4)	9023 (13)	0.41 (14)	23.
9'	16	V	2104 (8)	7019 (4)	8973 (13)	0.64 (15)	23.
10'	12	Ni	7103 (7)	0531 (3)	5940 (10)	0.12 (9)	28.
12	16	V	7321 (8)	3616 (4)	5822 (12)	0.39 (14)	23.
9	16	V	7303 (7)	6920 (3)	5825 (12)	0.07 (12)	23.
13	12	Ni	1487 (5)	0291 (3)	1516 (9)	-0.04 (8)	28.
17'	12	Ni	1195 (5)	3517 (3)	1441 (8)	0.32 (10)	28.
16'	12	Ni, Si	1251 (6)	7034 (3)	1507 (3)	0.01 (10)	26.2
13*	12	Si	7866 (11)	0357 (5)	0491 (17)	0.17 (19)	14.
(27	14	V	7340 (7)	4316 (3)	1171 (10)	-0.16 (10)	24.2)
(15'	14	V	7198 (7)	7623 (3)	1114 (10)	-0.40 (10)	23.2)
14'	14	V	8799 (7)	0655 (3)	5174 (11)	0.05 (10)	25.5
3	12	Ni	9025 (7)	4153 (3)	5346 (10)	0.10 (9)	28.
21	12	Ni	8885 (6)	7522 (2)	5340 (10)	-0.05 (8)	28.
(22'	14	V	8772 (8)	0922 (4)	2782 (13)	0.75 (14)	23.)
17	12	Si	8218 (10)	3599 (6)	3313 (16)	0.10 (20)	14.
16	12	Si	8251 (12)	6937 (7)	3329 (18)	0.72 (24)	14.
24	12	Si	0598 (11)	0494 (6)	6927 (16)	-0.10 (18)	14.
6'	12	Si	0538 (11)	3821 (5)	6937 (16)	-0.09 (18)	14.
28'	12	Si	0493 (9)	7276 (4)	6803 (14)	-0.74 (15)	14.
24'	16	V	8767 (8)	0310 (4)	8056 (13)	0.56 (13)	23.
6	12	Ni	9017 (7)	3824 (3)	7946 (10)	0.36 (10)	28.
28	12	Ni	8947 (7)	7199 (3)	7952 (10)	0.52 (10)	28.
27	14	V	2340 (7)	0684 (3)	6171 (10)	-0.16 (10)	24.2
23'	12	Ni	2059 (7)	3858 (3)	6071 (10)	0.19 (9)	28.
15'	14	V	2198 (7)	7377 (3)	6114 (10)	-0.40 (10)	23.2
27'	12	Ni	7062 (7)	0864 (3)	8537 (12)	0.71 (11)	28.
23	14	V	7342 (9)	4032 (4)	8737 (13)	1.00 (15)	23.7
15	14	V	7227 (9)	7331 (4)	8723 (13)	0.78 (14)	23.

Table 4. Range of interatomic distances in the *I* phase (Å)

The standard deviations are estimated to range from 0.009–0.032 Å.

CN	Atom No.	Occu-pancy	Distance range to near neighbors		CN	Atom No.	Occu-pancy	Distance range to near neighbors		CN	Atom No.	Occu-pancy	Distance range to near neighbors		
			Smallest distance	Largest distance				Smallest distance	Largest distance				Smallest distance	Largest distance	
16	1'	V	2.599	2.946	14	14'	V	2.222	2.940	12	27'	Ni	2.214	2.780	
	5'	V	2.629	2.946		15	V	2.252	2.990		28	Ni	2.159	2.756	
	7	V	2.601	2.988		15'	V	2.252	3.006		29	Ni	2.293	2.838	
	7'	V	2.646	2.982		22'	V	2.222	2.936		30	Ni	2.186	2.793	
	9	V	2.638	2.967		23	V	2.276	3.008		4'	Si	2.214	2.871	
	9'	V	2.669	2.998		27	V	2.276	3.022		5	Si	2.303	2.884	
	10	V	2.614	3.022		12	2	Ni	2.256		2.850	6'	Si	2.278	2.885
	11	V	2.620	3.006			3	Ni	2.303		2.775	13*	Si	2.226	2.857
	11'	V	2.529	2.999			4	Ni	2.348		2.807	16	Si	2.115	2.998
	12	V	2.647	2.979			6	Ni	2.115		2.740	17	Si	2.159	2.918
	19	V	2.624	2.879			8	Ni	2.280		2.769	20'	Si	2.289	2.818
	24'	V	2.660	2.940			10'	Ni	2.324		2.732	22	Si	2.210	2.879
	15	1	V	2.614			2.850	13	Ni		2.210	2.903	24	Si	2.257
8'		V	2.566	2.970	17'		Ni	2.131	2.759	26	Si	2.265	2.961		
12'		V	2.498	2.933	20		Ni	2.320	2.823	28'	Si	2.131	2.794		
18		V	2.501	2.838	21		Ni	2.299	2.729	3'	Ni, Si	2.256	2.848		
18'		V	2.498	2.925	21'		Ni	2.288	2.814	14	Ni, Si	2.234	2.819		
19'		V	2.566	2.936	23'		Ni	2.242	2.812	16'	Ni, Si	2.265	2.944		
					25		Ni	2.343	2.748	25'	Ni, Si	2.186	2.887		
					26'	Ni	2.300	2.833							

negative  $B$  values probably result from inaccuracies in the data set, neglect of absorption, and/or inadequacy of the scattering factors used. The occupancies in a ternary alloy cannot be unambiguously determined by an X-ray experiment alone, but the results are consistent with the following distribution of the atoms. This distribution has been formulated to be consistent with the results of determinations of many other t.c.p. structures, which have shown that elements to the left of Mn in the periodic table strongly prefer CN 14, CN 15, and CN 16, while those to the right, plus silicon, strongly prefer CN 12. The 12 CN 16 positions are assumed to be occupied by V only. One of the six CN 15 positions (19') has a negative  $B$  ( $< 2\sigma$ ) which might indicate that some Ni is present. Variation of  $m$  and  $B$  simultaneously, however, did not result in an occupancy significantly larger than one. Of the six CN 14 atoms four have occupancy factors larger than one, but not by significant amounts. Two of these atoms (15' and 27) have also negative  $B$ 's. Of the 33 CN 12 atoms 18 are Ni atoms (two, atoms 13 and 21, with very small negative  $B$ ), 11 are Si atoms and 4 are mixtures of Ni and Si. The Si atoms are less well defined than the heavier Ni and V atoms, a fact that shows up in the large range of  $B$  values. Atom 5 had a high negative  $B$  and occupancy of about 0.7 in an earlier stage of the refinement, but fixing the occupancy at unity resulted in a  $B$  value of about 0. During the cycles restricted to data with  $I > 2\sigma$ , atom 20' tried to escape from the structure ( $m = 0.08$ ). It was kept in the structure in the subsequent cycles based on all the data, whereupon  $m$  stabilized at 1.00 (13), while  $B$  at 3.35 (49) Å<sup>2</sup> was still

increasing ( $\Delta B \approx \sigma$ ) when the refinement was terminated. Atom 28' has a very large negative  $B$  [ $-0.74$  (15) Å<sup>2</sup>], with  $m = 1$ . Of the four mixtures two positions (3' and 14) are occupied by about 50% Ni and 50% Si, atom 16' is mainly Ni, and atom 25' is mainly Si. (These last two atoms are neighbors; see below.) The above distribution of the atoms yields, per asymmetric unit, 24 V, 20.1 Ni, and 12.9 Si; this is in good agreement with the stated composition of the alloy,  $V_{41}Ni_{36}Si_{23}$ , or, per asymmetric unit, 23.4 V, 20.5 Ni, and 13.1 Si.

### Description of the structure

The *I* phase structure is an 'ideally' t.c.p. structure that consists of ruffled layers stacked together; other such structures are the *R* phase (Komura, Sly & Shoemaker, 1960; Shoemaker & Shoemaker, 1978), the  $\delta$  phase (Shoemaker & Shoemaker, 1963), and the *K* phase (Shoemaker & Shoemaker, 1977). Only the 'regular' CN polyhedra occur; per asymmetric unit there are 12 of CN 16, 6 of CN 15, 6 of CN 14 and 33 of CN 12. All 'bonds' are five- or six-coordinated (*i.e.* the 'surface CN' of atoms on the polyhedra is everywhere 5 or 6), and all interstices are tetrahedral. The distances cover a range of 2.12–3.02 Å (Table 4) and follow the same dependence on CN as found before for t.c.p. structures.

The structure will be described in terms of the stacking of ruffled layers consisting of pentagons and triangles. There is a certain degree of arbitrariness in

deciding what atoms belong to the layers themselves and what atoms are 'subsidiary' atoms in between, because of the rumpling. However, the formulation presented here has a pleasing degree of self-consistency and is helpful in describing this extremely complicated structure.

### The pseudo repeat

In Table 3 the atoms are listed in groups of three with almost the same  $x$  and  $z$ , but with  $y$  coordinates differing by about  $\frac{1}{4}$ . Fig. 1 shows how these atoms are arranged in three layers, which are centered at about  $y = \frac{1}{24}$ ,  $\frac{9}{24}$ , and  $\frac{17}{24}$ . Primed (shown *double-primed* in Figs. 1–4) and unprimed atoms of the same number were related by a twofold axis in the model in  $C2/c$ ; atoms 2, 29 and 30 were on a twofold axis. The figure shows that the layers at  $\frac{9}{24}$  and  $\frac{17}{24}$  are very similar indeed, except for the puckering, the differences in the CN, and the kinds of atoms. The layer at  $\frac{1}{24}$  seems to be considerably different, particularly in the area including atom 13\*. If, however, one shifts this layer such that atom 13\* corresponds with atom 17' on the next layer, atom 8 with 20', atom 13 with atom 29, *etc.*, then the layers are practically identical except for the puckering.

### The stacking of the layers

The asymmetric unit consists of three layers between  $y = 0$  and  $\frac{1}{4}$ , namely layers at approximately  $\frac{1}{24}$ ,  $\frac{3}{24}$  and  $\frac{5}{24}$ , together with the 'subsidiary' atoms above these layers. The layer at  $\frac{3}{24}$  is related to the one at  $\frac{1}{24}$  shown in Fig. 1(b) by the operation of the  $n$  glide at  $y = \frac{1}{4}$ . The layer at  $\frac{5}{24}$  is related to the one at  $\frac{17}{24}$  shown in Fig. 1(c) by the  $C$  centering. Fig. 2 shows how the different layers stack together. Each layer is shown twice, once with an adjacent layer above it, and once with the other adjacent layer below it. (The layer at  $-\frac{1}{24}$  is related to the one at  $\frac{1}{24}$  by the  $c$  glide at  $y = 0$ , and the layer at  $\frac{23}{24}$  is related to the one at  $\frac{5}{24}$  by the  $n$  glide at  $y = \frac{1}{4}$ ; the asymmetric unit is contained between these two glide planes.) Thus, the coordinations of all the atoms are represented in Fig. 2.

The stacking principles are the same throughout the structure. Almost planar pentagons stack on top of each other antisymmetrically, thus largely defining icosahedra, *e.g.* those centered by atoms 3, 3', 14 and 27' in Fig. 2(b), and by atoms 21 and 21' in Fig. 2(d). An atom considerably displaced by rumpling from the plane of one layer fits over or under the center of a pentagon of an adjacent layer. This centering atom has CN 16 or CN 15 depending on the rumpling of the layers and on the configuration of the atoms in the layer on the other side. For instance atoms 10 and 1 in the upper layer of Fig. 2(a) have very similar surroundings in that figure, but different in the layer

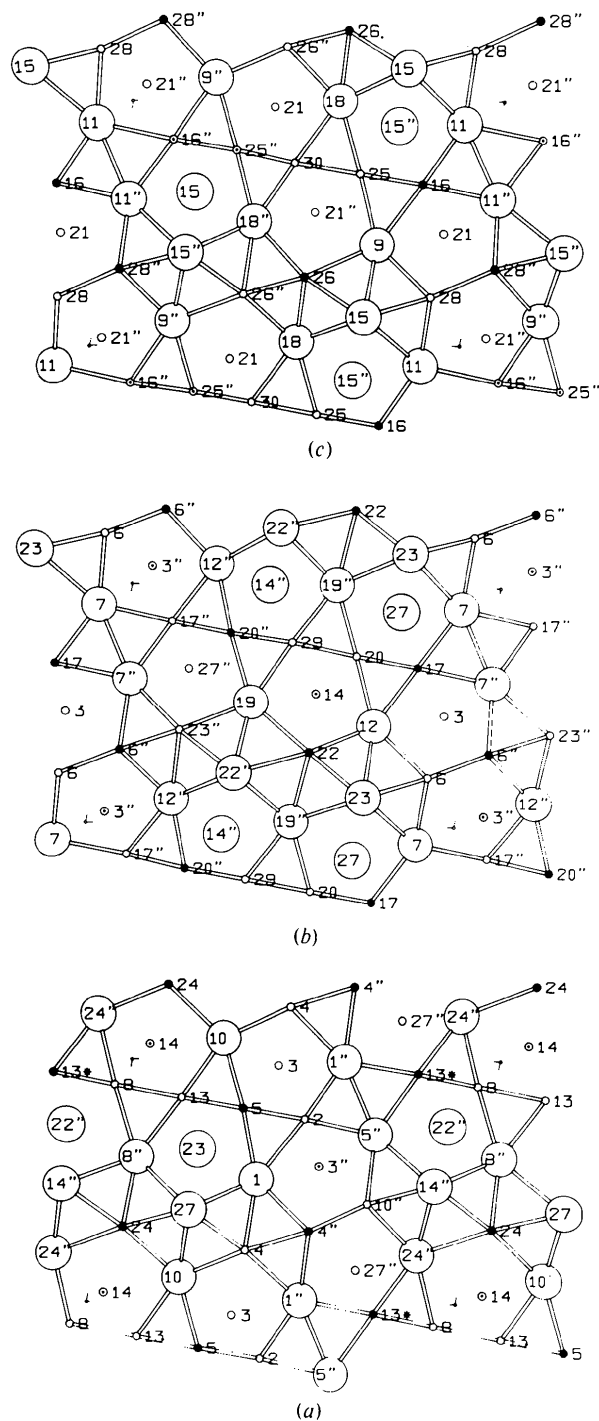


Fig. 1. *I* phase: ORTEP views (Johnson, 1976) in the direction of the  $-b$  axis of the three layers of crystallographically independent atoms which are separated by about one third of  $b$ . Layers are at approximately: (a)  $y = \frac{1}{24}$ , (b)  $y = \frac{9}{24}$ , (c)  $y = \frac{17}{24}$ . Atoms centering the pentagons are about  $\frac{1}{24}$  above the layers. Large circles are V atoms with CN 14, 15 or 16. Small circles are CN 12 atoms, representing Ni atoms when open, Si atoms when closed, and a mixture of Ni and Si when dotted at the center. The cell corners are indicated, the origin is at upper left,  $a$  is horizontal,  $c$  almost vertical. (Double primes in the figures correspond to single primes in the text.)

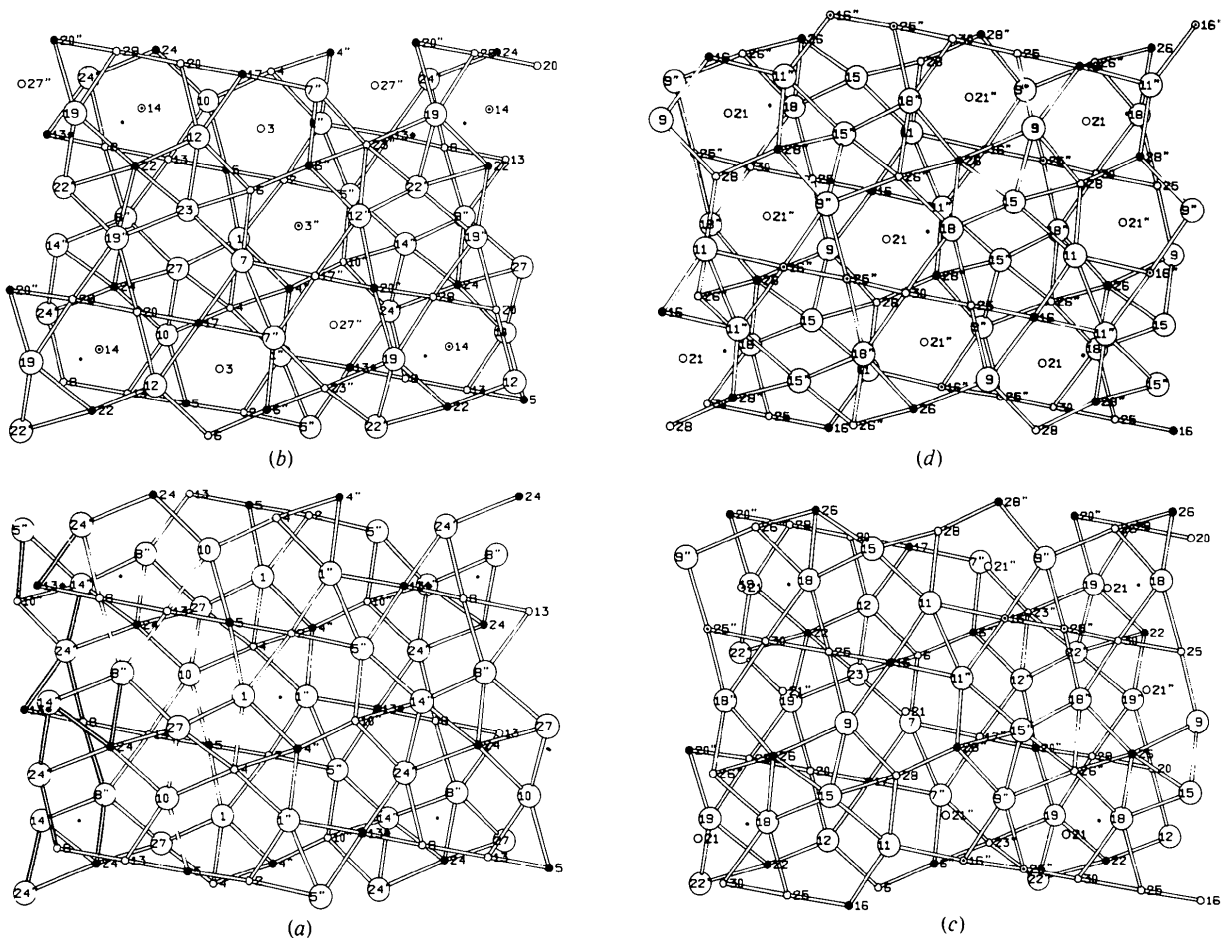


Fig. 2. I phase: ORTEP II views in the direction of the  $-b$  axis of the layers at  $y =$  approximately: (a)  $-\frac{1}{24}$  and  $+\frac{1}{24}$ , (b)  $\frac{1}{24}$  and  $\frac{1}{24}$ , (c)  $\frac{1}{24}$  and  $\frac{3}{24}$ , and (d)  $\frac{5}{24}$  and  $\frac{7}{24}$ . The direction of the axes is as in Fig. 1. This figure in stereo form has been deposited (see deposition footnote).

above them [Fig. 2(b)], thus giving atom 10 CN 16, and atom 1 CN 15. In some cases the atoms centering the pentagons occur in pairs forming atoms of CN 14 [23 and 27, 14' and 22' in Fig. 2(b), 15 and 15' in Fig. 2(d)].

#### The pseudo symmetry elements

There are pseudo twofold axes at approximately the positions of atoms 2, 29 and 30, relating primed and unprimed atoms. Pseudo symmetry centers occur, for example, at  $y = 0$  between atoms 1 and 1', 8 and 8' [Fig. 2(a)], and at  $y = \frac{1}{4}$  between atoms 9 and 9', 15 and 15' [Fig. 2(d)]. [Half of the pseudo centers in Fig. 2(a) correspond to the dots defining the corners and the center of the cell face; in Fig. 2(d) these are shifted from the dots by  $\frac{1}{4}$  in  $x$ .] Many atoms related by these pseudo symmetry elements occur at approximately the correct position, but differ in CN and occupancy. The members of a pair differ in their CN when their

polyhedra include atoms 13 or 13\* (e.g. 5 has CN 12 and 5' CN 16). When both sites of a pair have CN 12, their occupancy may be different [in Fig. 2(b) 6 is Ni and 6' is Si]. See also Table 4.

#### The distribution of the Si atoms

Fig. 1 shows that the distribution of the Si atoms (closed circles) in or near the layers is such that no two Si atoms are neighbors. Some Si positions are, however, adjacent to positions occupied by mixtures (circles centered by dots): in Fig. 1(a) atoms 24 and 14, 4' and 3', and in Fig. 1(b) atoms 22 and 14. Fig. 2 shows that the stacking maintains this distribution of the Si atoms: again no Si-Si contacts occur, but Si-mixture contacts occur [in Fig. 2(d) 26 and 16', in Fig. 2(c) 6' and 16', in Fig. 2(b) 6' and 3']. Atom 25', which is 79% Si, does not contact any Si atom; the mixture which it contacts, atom 16', is only 13% Si [Fig. 1(c)].

*The correspondence with the  $\mu$  phase and the major network*

Another view of the structure is given in Fig. 3, which is perpendicular to a slice parallel to (204). The 204 reflection is the strongest reflection observed, and was assumed to correspond to one of the strong (110)<sub>hex</sub> reflections in the  $\mu$  phase, caused by planes of atoms arranged in pentagons and triangles (Shoemaker & Shoemaker, 1967). Fig. 3 shows that the arrangement of the atoms in the *I* phase is quite different. There are approximately planar layers in this direction, but they form triangles, pentagons and hexagons. (In the slab shown all types of atoms occur at least once.) The closest similarity with the  $\mu$  phase is that, corresponding with the 12 layers perpendicular to the hexagonal *c* axis in the  $\mu$  phase, there are 12 layers perpendicular to **b** in the *I* phase. However, the layers are quite different (hexagons and triangles in  $\mu$ ,

pentagons and triangles in *I*; some layers are planar in  $\mu$ , none are in *I*).

Fig. 4 shows the atoms with CN > 12 and the six-coordinated 'major' bonds between them in a slab corresponding to the slab in Fig. 3, but 9 Å thick. The 'major network' formed by these bonds consists of interconnected corrugated layers of hexagons formed by CN 15 and CN 16 atoms, with rows of CN 14 atoms between them. In the  $\mu$  phase the CN 15 atoms form a network of six-membered rings, but it is planar and occurs perpendicular to the hexagonal *c* axis (corresponding with the long axis in Fig. 4).

### Conclusion

The *I* phase appears to be one of the most complex intermetallic structures ever determined, exceeded perhaps only by structures with very large unit cells and high symmetry but with fewer positional parameters than the *I* phase structure (e.g. Cu<sub>4</sub>Cd<sub>3</sub>, Samson, 1967). The complexity of the structure may derive in part from the tendency of the Si atoms to avoid each other. We have also observed such behavior in the *K* phase (Shoemaker & Shoemaker, 1977). In that structure there is a subcell in which CN 12 sites are occupied by mixtures of Mn and Si, and there is a supercell with one doubled dimension, which is apparently caused by the ordering of the Mn and Si atoms on corresponding sites in the two subcells, such that no Si-Si contacts occur. The mechanism of the stabilization of t.c.p. phases by Si is not understood, but it may well be of electronic origin; Si atoms may be charged and thus avoid each other. In the *I* phase we observe for the first time adjacent sites occupied by Si and mixtures, which may well mean that the limit of the Si content in ideally t.c.p. phases is approaching at the composition of the *I* phase. Bardos & Beck (1966) report that the *I*-phase field in the V-Ni-Si system extends to about 27 at.% Si. If all the Ni, Si mixture positions are occupied by Si, the Si content will be 26.3 at.%. The Si atoms will then have from one to three Si neighbors. No ideally t.c.p. structures have been reported with higher than 26 at.% Si (Kripyakevich & Yarmolyuk, 1970).

We wish to thank Professor Paul A. Beck of the University of Illinois for providing a sample of the *I* phase. We are grateful to Dr Ted E. Hopkins of Oregon State University for assistance with the computer programs *MULTAN* and *ORTEP II* and to Mrs Rita Hazell of Århus University for suggesting modifications in *MULTAN*. We thank Dr A. Zalkin of the Lawrence Berkeley Laboratory for making available to us his system of programs on the CDC 7600 computer. We gratefully acknowledge the financial support of the National Science Foundation.

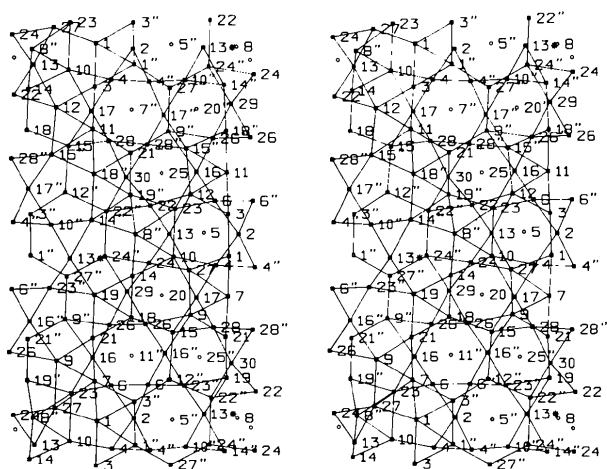


Fig. 3. *I* phase: ORTEP perpendicular stereoview of a slice of the structure 3.40 Å thick, centered at 0.542, 0.5, 0.369, parallel to (204). The *b* axis is vertical in the paper.

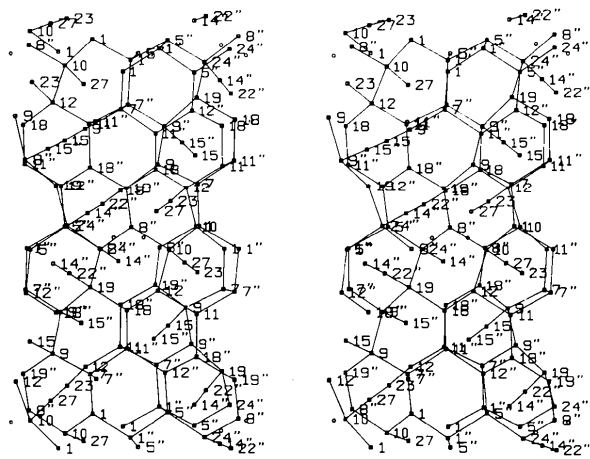


Fig. 4. *I* phase: ORTEP stereoview as in Fig. 3 showing only the atoms with CN > 12 and the six-coordinated bonds between them forming the 'major network'. The center of the slice is as in Fig. 3, the thickness is 9 Å.

## References

- BARDOS, D. I. & BECK, P. A. (1966). *Trans. Am. Inst. Min. Metall. Pet. Eng.* **236**, 64–69.
- BARDOS, D. I., MALIK, R. K., SPIEGEL, F. X. & BECK, P. A. (1966). *Trans. Am. Inst. Min. Metall. Pet. Eng.* **236**, 40–48.
- CROMER, D. T. & LIBERMAN, D. (1970). *J. Chem. Phys.* **53**, 1891–1898.
- International Tables for X-ray Crystallography* (1962). Vol. III. Birmingham: Kynoch Press.
- JOHNSON, C. K. (1976). *ORTEP-II*. Report ORNL-3794. Oak Ridge National Laboratory, Tennessee.
- KOMURA, Y., SLY, W. G. & SHOEMAKER, D. P. (1960). *Acta Cryst.* **13**, 575–585.
- KRIPYAKEVICH, P. I. & YARMOLYUK, Y. P. (1970). *Dopov. Akad. Nauk Ukr. RSR, Ser. A*, **32**, 948–951.
- KUZMA, YU. B. & HLADYSHEVSKII, E. I. (1964). *Zh. Neorg. Khim.* **9**, 674–681.
- KUZMA, YU. B., HLADYSHEVSKII, E. I. & CHERKASHIN, E. E. (1964). *Zh. Neorg. Khim.* **9**, 1898–1904.
- MAIN, P., HULL, S. E., LESSINGER, L., GERMAIN, G., DECLERCQ, J. P. & WOOLFSON, M. M. (1978). *MULTAN 78. A System of Computer Programs for the Automatic Solution of Crystal Structures from X-ray Diffraction Data*. Univs. of York, England, and Louvain, Belgium.
- MANOR, P. C., SHOEMAKER, C. B. & SHOEMAKER, D. P. (1972). *Acta Cryst.* **B28**, 1211–1218.
- SAMSON, S. (1967). *Acta Cryst.* **23**, 586–600.
- SHOEMAKER, C. B. & SHOEMAKER, D. P. (1963). *Acta Cryst.* **16**, 997–1009.
- SHOEMAKER, C. B. & SHOEMAKER, D. P. (1967). *Trans. Am. Inst. Min. Metall. Pet. Eng.* **239**, 937–940.
- SHOEMAKER, C. B. & SHOEMAKER, D. P. (1976). *Acta Cryst.* **B32**, 2306–2313.
- SHOEMAKER, C. B. & SHOEMAKER, D. P. (1977). *Acta Cryst.* **B33**, 743–754.
- SHOEMAKER, C. B. & SHOEMAKER, D. P. (1978). *Acta Cryst.* **B34**, 701–705.
- YVON, K., JEITSCHKO, W. & PARTHÉ, E. (1969). *A Fortran IV Program for the Intensity Calculation of Powder Patterns*. Univ. of Pennsylvania.
- ZACHARIASEN, W. H. (1963). *Acta Cryst.* **16**, 1139–1144.

*Acta Cryst.* (1981). **B37**, 8–11

## The Structure of $N_2$ at 49 kbar and 299 K\*

BY DON T. CROMER, ROBERT L. MILLS, DAVID SCHIFERL AND LARRY A. SCHWALBE

*University of California, Los Alamos Scientific Laboratory, Los Alamos, NM 87545, USA*

(Received 8 February 1980; accepted 17 June 1980)

### Abstract

A single crystal of  $N_2$  at 49 kbar (4.9 GPa) and 299 K was produced in a Merrill–Bassett diamond-anvil high-pressure cell and examined by X-rays. Pressure was determined by the ruby-fluorescence method. The unit cell is cubic,  $a_0 = 6.164(1) \text{ \AA}$ , space group  $Pm\bar{3}n$ , with eight molecules per unit cell. The structure is the same as that of  $\beta\text{-F}_2$  and  $\gamma\text{-O}_2$  at 50 K and atmospheric pressure. For seven refined parameters and 19 observations the final  $R_w$  is 0.0488.

### Introduction

As a continuation of studies of  $N_2$  at high pressure (Schuch & Mills, 1970; Mills, Liebenberg & Bronson, 1975; Schiferl, Cromer & Mills, 1978; Schwalbe, Schiferl, Mills, Jones, Ekberg, Cromer, LeSar & Shaner, 1980; LeSar, Ekberg, Jones, Mills, Schwalbe &

Schiferl, 1979), we made X-ray diffraction measurements on a single crystal of  $N_2$  in a diamond cell at 49 kbar and 299 K. The structure is the same as that of  $\beta\text{-F}_2$  (Jordan, Streib & Lipscomb, 1964) and  $\gamma\text{-O}_2$  (Jordan, Streib, Smith & Lipscomb, 1964; Cox, Samuelsen & Beckurts, 1973).

### Experimental

A Merrill–Bassett diamond-anvil cell (Merrill & Bassett, 1974), modified to utilize stronger beryllium pieces (Schiferl, 1977) and to provide uniform X-ray absorption and better optical access (Keller & Holzapfel, 1977), was loaded by total immersion in liquid  $N_2$  as described by Schiferl *et al.* (1978). Pressure was measured according to the ruby-fluorescence scale, assuming the  $R_1$  line shift to be given by the linear relation,  $d\lambda/dp = 0.365 \text{ \AA kbar}^{-1}$  (Forman, Piermarini, Barnett & Block, 1972; Barnett, Block & Piermarini, 1973).

Preparation of a single crystal for X-ray studies at 49 kbar was difficult because  $N_2$  undergoes a phase

\* Work performed under the auspices of the US Department of Energy.